



**HAL**  
open science

## Role of the cysteinyl residues in *Arabidopsis thaliana* cyclophilin CYP20-3 in peptidyl-prolyl cis-trans isomerase and redox-related functions

Miriam Laxa, Janine König, Karl-Josef Dietz, Andrea Kandlbinder

### ► To cite this version:

Miriam Laxa, Janine König, Karl-Josef Dietz, Andrea Kandlbinder. Role of the cysteinyl residues in *Arabidopsis thaliana* cyclophilin CYP20-3 in peptidyl-prolyl cis-trans isomerase and redox-related functions. *Biochemical Journal*, 2006, 401 (1), pp.287-297. 10.1042/BJ20061092 . hal-00478635

**HAL Id: hal-00478635**

**<https://hal.science/hal-00478635>**

Submitted on 30 Apr 2010

**HAL** is a multi-disciplinary open access archive for the deposit and dissemination of scientific research documents, whether they are published or not. The documents may come from teaching and research institutions in France or abroad, or from public or private research centers.

L'archive ouverte pluridisciplinaire **HAL**, est destinée au dépôt et à la diffusion de documents scientifiques de niveau recherche, publiés ou non, émanant des établissements d'enseignement et de recherche français ou étrangers, des laboratoires publics ou privés.

**Role of the cysteinyl residues in *Arabidopsis thaliana* cyclophilin CYP20-3 in peptidyl-prolyl *cis-trans* isomerase and redox-related functions**

Miriam Laxa<sup>\*</sup>, Janine König<sup>\*/†</sup>, Karl-Josef Dietz<sup>\*/‡</sup> and Andrea Kandlbinder<sup>\*</sup>

**Running title: *Arabidopsis thaliana* cyclophilin CYP20-3**

\* Biochemistry and Physiology of Plants, W5, Bielefeld University, 33501 Bielefeld

† Division of Biological Chemistry and Molecular Microbiology, The Wellcome Trust Biocentre, University of Dundee, Dundee DD1 5EH, UK

‡ Address for correspondence:

Biochemistry and Physiology of Plants

Faculty of Biology, W5

Bielefeld University

33501 Bielefeld

++49 521 106 5589

++49 521 106 6039

E-mail: karl-josef.dietz@uni-bielefeld.de

**Abstract**

1 Cyclophilins (CyPs) are ubiquitous proteins of the immunophilin superfamily with proposed  
2 functions in protein folding, protein degradation, stress response and signal transduction.  
3 Conserved Cys-residues further suggest a role in redox regulation. In order to get insight into  
4 the conformational change mechanism and functional properties of the chloroplast located  
5 CYP20-3, site-directed mutagenised Cys→Ser-variants were generated and analyzed for  
6 enzymatic and conformational properties under reducing and oxidising conditions. Compared  
7 to the wild type form elimination of three out of the four cysteinyl residues decreased the  
8 catalytic efficiency of peptidyl-prolyl *cis-trans* isomerase (PPI) activity of the reduced  
9 CYP20-3 indicating a regulatory role of dithiol-disulfide transitions in protein function.  
10 Oxidation was accompanied by conformational changes with a predominant role in the  
11 structural rearrangement of the disulfide bridge formed between Cys<sup>54</sup> and Cys<sup>171</sup>. The rather  
12 negative midpoint redox potential of -319 mV places CYP20-3 into the redox hierarchy of the  
13 chloroplast suggesting the activation of CYP20-3 in the light under condition of limited  
14 acceptor availability for photosynthesis as realised under environmental stress. Chloroplast  
15 peroxiredoxins (Prx) were identified as interacting partners of CYP20-3 in a DNA-protection  
16 assay. A catalytic role in the reduction of 2-Cys PrxA and B was assigned to Cys<sup>129</sup> and  
17 Cys<sup>171</sup>. In addition it was shown that the isomerisation and disulfide reduction activities are  
18 two independent functions of CYP20-3 that both are regulated by the redox state of its active  
19 centre.

20

21 **Key words:** *Arabidopsis thaliana*, cyclophilin, chloroplast, immunophilin, prolyl-peptidyl *cis-*  
22 *trans* isomerase, peroxiredoxin, redox regulation

23

24 **Abbreviations:** AMS: 4-acetoamido-4'-maleimidyl-stilbene-2,2'-disulfonate; Cyp:  
25 cyclophilin; DTT: dithiothreitol; H<sub>2</sub>O<sub>2</sub>: hydrogen peroxide; PPI: prolyl-peptidyl *cis-trans*  
26 isomerase; Prx: peroxiredoxin; RT: room temperature; WT: wild type.

27

## Introduction

1 Cyclophilins are members of the immunophilin protein superfamily. The *Arabidopsis* genome  
2 encodes at least 52 genes for immunophilins, immunophilin-like proteins and multidomain  
3 proteins with immunophilin domains [1]. Thus, plants possess the largest number of  
4 immunophilin family members as compared to other organisms with sequenced genomes at  
5 present [2]. Among these, 29 gene products belong to the cyclophilin (CYP) subfamily [3].  
6 The functions of the plant CYPs mostly are unknown and unexplored. In mammals they were  
7 first identified as targets of the immunosuppressive drug cyclosporin A [4]. They constitute a  
8 family of phylogenetically old proteins occurring ubiquitously in bacteria, animals and plants  
9 [1; 3; 5] where they are known for their function in the isomerisation of Xaa-Pro-peptide  
10 bonds during the folding and assembly of proteins. Furthermore they act as chaperones [6; 7;  
11 8; 9; 10; 11] and are involved in regulatory signal transduction pathways [2; 12; 13] during  
12 stress responses [14; 15; 16], plant development [17] and affect RNA splicing reactions [5;  
13 18; 19]. Lee et al. observed the binding of human CypA to human peroxiredoxins Prdx I-VI  
14 by MALDI-TOF analysis and confirmed it via protein overlay assays and subsequent Western  
15 immunoblot analysis [20]. Recently it was shown in a DNA protection assay that a  
16 cyclophilin from *Pisum sativum* is able to reduce oxidised 2-Cys Prx and regenerates the  
17 peroxide detoxifying activity [21]. The reaction mechanism is still unclear.

18 Plant peroxiredoxins are non-heme containing peroxidases [22; 23]. They detoxify hydrogen  
19 peroxide, alkyl hydroperoxides and peroxynitrite [24; 25; 26]. The active centre contains a  
20 conserved cysteinyl residue, which reduces different peroxides. Its regeneration is coupled to  
21 electron donors such as thioredoxins, glutaredoxins and cyclophilins [21; 26]. Prxs are  
22 grouped into four clans, namely 1-Cys Prx, 2-Cys Prx, type II-Prx und PrxQ, according to  
23 sequence similarities, presence of an additional resolving cysteinyl group at variable  
24 positions, as well as the mechanisms of catalysis and regeneration [23; 25]. The *Arabidopsis*  
25 *thaliana* genome encodes 10 different Prxs with distinct subcellular localisation, tissue  
26 distribution, transcriptional regulation and biochemical properties [22; 27]. Prxs play a role in  
27 the antioxidative protection system of photosynthesis, respiration and stress response.  
28 Additional functions are proposed in signal transduction during plant development and  
29 adaptation [25; 24; 27].

30 The 28.2 kDa cyclophilin CYP20-3 (at3g62030; Roc4) has been characterised previously. It is  
31 located in the stroma of chloroplasts [28; 29; 3] and the four conserved amino acids Arg<sup>69</sup>,  
32 Phe<sup>74</sup>, Trp<sup>135</sup>, His<sup>140</sup> (R-F-W-H-motive) are involved in peptidyl-prolyl-isomerase activity and

1 cyclosporin A-binding (Trp) implicating a function in protein folding. From transcript  
2 analyses, a role in protein unfolding and degradation has been proposed under stress  
3 conditions such as heat shock [3]. Additionally it was identified as a target protein for  
4 chloroplast Trx-m [30; 31]. CYP20-3 contains four cysteinyl residues, which form two  
5 disulfide bonds under oxidising conditions, namely Cys<sup>54</sup>-Cys<sup>171</sup> and Cys<sup>129</sup>-Cys<sup>176</sup>, indicating  
6 redox-dependent conformational changes shown by 5,5'-dithio-bis(2-nitrobenzoic acid)  
7 binding and MALDI-TOF mass spectrometry [31].

8 This study aims at improving our understanding of the recently found redox properties of  
9 CYP20-3 and its interaction with the different chloroplast located peroxiredoxins. To this end,  
10 each Cys-residue of CYP20-3 was mutagenised and the variants were heterologously  
11 expressed in *E. coli*. His-tagged variants as well as the wild type protein were analysed for  
12 peptidyl-prolyl *cis-trans* isomerase (PPI) activity, redox-dependent electrophoretic mobility  
13 using band shift-experiments as well as for their redox-dependent conformational changes by  
14 intrinsic Trp fluorescence analysis. The midpoint redox potential of wild type and variant  
15 proteins was determined to place CYP20-3 into the redox system of the plastids. Furthermore,  
16 the disulfide reducing property of CYP20-3 was analysed in DNA-protection assays with all  
17 four chloroplast located peroxiredoxins.

## Material and Methods

1 **RNA Isolation and cDNA Synthesis.** Total RNA was isolated from rosette leaves of  
2 *Arabidopsis thaliana* (ecotype Col-0) plants grown in soil culture (1:1:1 mixture of  
3 Frühsdorfer Erde Klocke P, perlite and vermiculite) in a controlled environment (10 h of light,  
4 100  $\mu\text{mol quanta m}^{-2} \text{s}^{-1}$ , 23°C and 14 h darkness at 18°C; 50% relative humidity) for 28-32  
5 days. The plant material was frozen in liquid nitrogen and ground to a fine powder. Total  
6 RNA was extracted using an RNA-isolation kit (Promega, Mannheim, D) according to the  
7 manufacturer's instructions. Following DNase I-treatment, cDNA was synthesised from 5  $\mu\text{g}$   
8 of total RNA with M-MLV RT II [H-] (Promega, Mannheim, D) and oligo-dT-priming in 30  
9  $\mu\text{l}$  reactions.

10 **Heterologous Expression and Site-Directed Mutagenesis of CYP20-3.** CYP20-3 was  
11 amplified from *Arabidopsis* cDNA without the N-terminal sequence encoding the signal  
12 peptide, using Pfu (*Pyrococcus furiosus*) polymerase (Stratagene, La Jolla, CA, USA). Site-  
13 directed mutations were introduced with two subsequent PCRs according to Montemartini et  
14 al. [32]. The primers used for mutagenesis are listed in the supplementary table S1. CYP20-3  
15 cDNA was cloned into the pCR<sup>®</sup>T7/NT-Topo<sup>®</sup> vector and transformed into BL21(DE3)pLysS  
16 cells (Invitrogen, La Jolla, CA, U) for heterologous expression of wild type and variants of  
17 CYP20-3 as His-tagged fusion proteins. The mutations were verified by sequencing.

18 **Culture Growth and Purification of His-tagged Proteins.** 2 l LB medium containing 100  
19  $\mu\text{g/ml}$  ampicillin was inoculated with 150 ml of a non-induced overnight bacteria culture and  
20 incubated at 37 °C until an optical density of 0.6 – 0.8 was reached at 600 nm using a  
21 spectrophotometer (Uvikon 930, Kontron-Instruments). Expression of recombinant protein  
22 was induced by addition of isopropyl-1-thio- $\beta$ -D-galactopyranoside to a final concentration of  
23 0.4 mM. After 4 h, the cells were harvested by centrifugation (4000 x g, for 30 min at 4°C)  
24 and the cell pellet was stored overnight at -20 °C. Heterologously expressed proteins [CYP20-  
25 3<sub>WT</sub>, CYP20-3<sub>C54S</sub>, CYP20-3<sub>C129S</sub>, CYP20-3<sub>C171S</sub> and CYP20-3<sub>C176</sub> and CYP20-3 <sub>$\Delta$ PPI</sub>] were  
26 purified as described previously [33] either under reducing (10 mM  $\beta$ -mercaptoethanol in the  
27 lysis buffer) or non-reducing (no reducing reagent) conditions as indicated. The protein  
28 concentrations were determined spectrophotometrically using the Bio-Rad protein assay  
29 (BioRad, München D) using bovine serum albumine as a tentative reference. The protein was  
30 stored at -80° C. *E. coli* Trx was overexpressed and purified as described by Yamamoto *et al.*  
31 [34], 2-Cys PrxA, 2-Cys PrxB, PrxII E and PrxQ according to Horling *et al.* [22]. Trx y1 was  
32 kindly provided by Dr. Emmanuelle Issakidis-Bourguet and Dr. Myroslawa Miginiac-Maslow

1 [35].

2 **Electrophoretic mobility.** A typical assay (50  $\mu$ l) consisted of 40 mM potassium-phosphate  
3 buffer (pH 7.0), 1.25  $\mu$ g Cyp protein, various concentrations of H<sub>2</sub>O<sub>2</sub> and DTT (1-10 mM).  
4 Following incubation for 15 min at room temperature, the samples were supplemented with  
5 equal volumes of 3x-concentrated non-reducing loading buffer (375 mM Tris-HCl, pH 6.8, 30  
6 % glycerin, 12 % SDS, 0.03 % bromophenol blue), and 20  $\mu$ l aliquots each separated on a  
7 SDS-16% PAGE. Proteins were detected by silver staining.

8 **Excitation and Emission Spectrum of Trp Fluorescence.** 2  $\mu$ M Cyp protein dissolved in  
9 phosphate-buffered saline pH 7.0 (137.0 mM NaCl, 18.8 mM Na<sub>2</sub>HPO<sub>4</sub>; 2.7 mM KCl; 2.0  
10 mM KH<sub>2</sub>PO<sub>4</sub>) was incubated either with 10 mM DTT or 20 mM H<sub>2</sub>O<sub>2</sub> for 5 min at RT.  
11 Excitation and emission spectra were obtained using a spectrofluorimeter (SFM 25, Kontron-  
12 Instruments). Trp fluorescence was excited at a wavelength of 290 nm and the emission  
13 spectrum was recorded as relative fluorescence over a range from 300 – 400 nm. At least 9  
14 independent measurements were carried out for each sample. Data were fitted with the  
15 software program FindGraph using an asymmetric Gauss equation.

16 **Peptidyl-Prolyl cis-trans Isomerisation Assay.** The PPI assay was performed as described  
17 previously [36] with minor modifications. A 1-ml assay consisted of 35 mM Hepes buffer  
18 (pH 8.0), 250  $\mu$ g  $\alpha$ -chymotrypsin (Sigma), 75 nM Cyp, 100  $\mu$ M N-succinyl-Ala-Ala-Pro-Phe-  
19 *p*-nitroanilide (Sigma, Deissenhofen D) as chromogenic substrate (10 mM stock solution was  
20 dissolved in 100% methanol) and either 10 mM DTT (AppliChem, Darmstadt D) or 2.5 mM  
21 H<sub>2</sub>O<sub>2</sub> (Roth). All components of the assay mixture except the  $\alpha$ -chymotrypsin were combined  
22 and preincubated at 10°C for 10 min.  $\alpha$ -Chymotrypsin was added and quickly mixed to  
23 initiate the reaction. The absorbance was read every 6 s over a period of 5 min at 390 nm  
24 using a spectrophotometer (Uvikon 930, Kontron-Instruments). Data were fitted to a first-  
25 order rate equation ( $A_{360} = A_1 + A_0e^{-kt}$ , with  $k$  as rate constant) and rate constants ( $k_{obs}$ ) derived  
26 as described by Motohashi et al. [31]. The  $k_{cat}/K_m$  values were calculated according to the  
27 equation  $k_{cat}/K_m = (k_{obs} - k_0)/[PPIase]$ , where  $k_0$  is the first-order rate constant for  
28 spontaneous *cis-trans* isomerisation [37].

29 **Oxidation-Reduction Midpoint Potential.** Recombinant CYP20-3 was titrated at pH 7.0.  
30 After 3 h incubation in MOPS buffer (100 mM) containing 2 mM total DTT (in different  
31 ratios of reduced and oxidised DTT) at ambient temperature, the reduced fraction of Cyp was  
32 labelled with monobromobimane (10 mM) and analysed for fluorescence [38]. Data were  
33 fitted with the software program GraFit5 using the Nernst equation with  $n = 4$  (in case of

1 CYP20-3<sub>WT</sub>) and n = 3 (for each mutant protein as one cysteine was missing) based on a value  
2 of -330 mV for the Em of DTT at pH 7.0.

3 **DNA-Protection Assay.** CYP20-3-dependent reduction of recombinant chloroplastidic Prx  
4 was tested in a DNA-cleavage assay as described previously [21] with minor modifications.  
5 ROS production was induced by incubation of 3  $\mu$ M FeCl<sub>3</sub> in the presence of 10 mM DTT for  
6 3 h at 37 °C. Supercoiled plasmid DNA (pCR<sup>®</sup>T7/NT-Topo<sup>®</sup> vector; 2  $\mu$ g) was added and  
7 incubated for 5 h at 37 °C. The reaction contained 6  $\mu$ g Prx protein and 3  $\mu$ g CYP20-3 or Trx  
8 protein as indicated. The *Arabidopsis* peroxiredoxin proteins, 2-Cys PrxA and 2-Cys PrxB,  
9 PrxII E and PrxQ [22] were preincubated with 5 mM DTT for 5 min followed by incubation  
10 with 20 mM H<sub>2</sub>O<sub>2</sub> for 1 h, CYP20-3<sub>WT</sub> with either 10 mM DTT or 10 mM H<sub>2</sub>O<sub>2</sub> for 1 h. The  
11 proteins were dialysed overnight against 40 mM potassium-phosphate buffer (pH 7.0).  
12 Nicking and fragmentation of supercoiled plasmid DNA were monitored by gel  
13 electrophoresis in a 1% agarose gel.

## Results

14 **Generation of CYP20-3<sub>WT</sub> and Variants.** Site-directed mutations were introduced in the  
15 primary aa sequence to investigate the functional significance of the Cys residues in CYP20-  
16 3. Overexpressed N-terminally His-tagged CYP20-3<sub>WT</sub> and variants were isolated and  
17 purified by Ni-NTA chromatography with yields of 0.25 to 2 mg/l *E. coli* culture. In non-  
18 reducing SDS-PAGE separations, CYP20-3<sub>WT</sub> and all variants with the exception of CYP20-  
19 3<sub>C54S</sub> were detected as reduced monomers after purification under reducing conditions (Figure  
20 1A-E, 1<sup>st</sup> lane). CYP20-3<sub>C176S</sub> revealed a doublet band with a predominant form of lower  
21 electrophoretic mobility indicating a partially abnormal conformation, while in wild type  
22 protein, the faster migrating form was abundant. Following purification under non-reducing  
23 conditions, CYP20-3<sub>C176S</sub> was detected as a dimer (Figure 1F).

24  
25 **Redox-Dependent Electrophoretic Mobility of the SDS-Solubilized Proteins under Oxidising  
26 and Reducing Conditions.** As reported by Motohashi et al. [31] two disulfide bonds (Cys<sup>54</sup> –  
27 Cys<sup>171</sup> and Cys<sup>129</sup> – Cys<sup>176</sup>) can be formed in CYP20-3<sub>WT</sub> that are sensitive to the redox  
28 milieu as shown by AMS-labelled protein mobility on SDS-PAGE. Thiol/disulfide transitions,  
29 e.g. by generating a more compact structure through an intramolecular disulfide bridge  
30 formation, often alter apparent electrophoretic mobilities of proteins. Therefore, the CYP20-  
31 3<sub>WT</sub> and the diverse variants were checked under oxidising and reducing conditions. In the

1 presence of H<sub>2</sub>O<sub>2</sub> CYP20-3<sub>WT</sub> showed a higher mobility than after treatment with DTT  
2 (Figure 1A). Interestingly, the CYP20-3<sub>C176S</sub> protein showed aberrant mobility compared to  
3 the wild type and all other Cys→Ser variants. The observed difference in electrophoretic  
4 mobility between both monomeric forms was considerably larger than that between the  
5 reduced and oxidised forms of the wild type protein. CYP20-3<sub>C176S</sub> was partially oxidised  
6 after purification, separated as doublet band and showed no further conformational change  
7 upon addition of hydrogen peroxide (Figure 1E). The purification under non-reducing  
8 conditions of CYP20-3<sub>C176S</sub> showed a dimeric form of this variant that converted to the  
9 doublet monomeric form upon DTT treatment (Figure 1F). CYP20-3<sub>C54S</sub> existed in an  
10 oxidised and reduced form, but the presence of the oxidised form after purification under  
11 reducing conditions indicates that the reduced form is not stable and highly sensitive to  
12 oxidation (Figure 1B). The disulfide bond between Cys<sup>129</sup> and Cys<sup>176</sup> forms spontaneously.  
13 The deletion of either Cys129 or Cys176 that form a disulfide bond in the oxidised protein  
14 [31] caused no conformational changes if purified under reducing conditions. Compared to  
15 the wild type protein CYP20-3<sub>C171S</sub> is also less sensitive towards hydrogen peroxide,  
16 suggesting that no stable disulfide bridge is formed as Cys<sup>54</sup> sterically inhibits the  
17 spontaneous formation of the disulfide bond between Cys<sup>129</sup> and <sup>176</sup> (see below, Figure 6A).  
18 Formation of a disulfide bond between the adjoining Cys<sup>54</sup> and Cys<sup>176</sup> in the tertiary structure  
19 can be excluded. On the contrary, CYP20-3<sub>C129S</sub> and CYP20-3<sub>C171S</sub> were detected mostly in  
20 the reduced form and their mobility was not altered under oxidising conditions (Figure 1C,  
21 D). This observation indicates that major intramolecular changes associated with the  
22 transition from the reduced to the oxidised molecule were absent and probably no disulfide  
23 bonds were formed in these variants (Figure 1C, D). Apparently, both disulfide bonds are  
24 necessary to stabilise the conformation of the oxidised CYP20-3 molecule. These results  
25 support the hypothesis that the transition from the reduced to the oxidised form of CYP20-3  
26 as well as the stability of the oxidised form depend on the formation of both disulfide bonds.  
27 Furthermore, the two disulfide bonds appear to be formed in a coordinated and ordered way.

28

29 *Intrinsic Fluorescence Reveals Conformational Changes during the Transition from the*  
30 *Reduced to the Oxidised State.* Analysis of the intrinsic fluorescence offers a powerful  
31 approach for studying conformational changes in proteins. The aromatic amino acid  
32 tryptophan is rather specifically excited at a wavelength of 290 nm [39]. Burstein et al. (1973)  
33 [40] introduced two different classes of emission spectra equivalent to different Trp locations  
34 within the protein structure. The class I-Trp is characterised by  $\lambda_{em-max}=330-332$  nm

1 corresponding to a location in the interior of the protein, being shielded from the solvent,  
2 whereas class II-Trp residues are exposed to the solvent at the protein surface with  $\lambda_{em-}$   
3  $\lambda_{em-max}=340-342$  nm. CYP20-3 contains one Trp residue (Trp<sup>135</sup>) which is part of the R-W-F-H-  
4 motif and located close to the surface of the protein in the vicinity of Cys<sup>129</sup> (Figure 6A, B).  
5 Emission spectra of CYP20-3<sub>WT</sub> and its Cys-variants were compared under oxidising and  
6 reducing conditions. For CYP20-3<sub>WT</sub> a blue shift of  $\lambda_{em-max}$  of 1.6 nm occurred during  
7 transition from reducing to oxidising conditions indicating that Trp<sup>135</sup> is more shielded from  
8 the solvent in the presence of H<sub>2</sub>O<sub>2</sub> (Figure 2A, Table 1). In the presence of DTT the  
9 maximum Trp<sup>135</sup>- fluorescence was blue-shifted in all Cys→Ser variants compared to the wild  
10 type with exception of the CYP20-3<sub>C129S</sub>, whereas in the presence of H<sub>2</sub>O<sub>2</sub> the fluorescence  
11 maximum was either blue-shifted in CYP20-3<sub>C54S</sub> and CYP20-3<sub>C176S</sub> or red-shifted in CYP20-  
12 3<sub>C129S</sub> and CYP20-3<sub>C171S</sub> (Figure 2, Table 1). Interestingly, the fluorescence emission spectra  
13 of the variants mutated in the interacting disulfide bond partners were similar (Figure 2).  
14 While  $\lambda_{em-max}$  of CYP20-3<sub>C54S</sub> and CYP20-3<sub>C171S</sub> was red-shifted by 2.7 and 2.8 nm,  
15 respectively, upon oxidation only a slight shift in maximum fluorescence  $\lambda_{em-max}$  was observed  
16 for CYP20-3<sub>C129S</sub> as well as CYP20-3<sub>C176S</sub> (Figure 2, Table 1). This indicates either an  
17 increased exposure of Trp<sup>135</sup> to the solvent or a stimulated quenching effect of Cys<sup>129</sup> in the  
18 oxidised form. In case of CYP20-3<sub>C129S</sub> only a slight shift in the fluorescence maximum by  
19  $\lambda_{em-max} = 344.1$  nm (red) and  $\lambda_{em-max} = 344.9$  nm (ox) was observed indicating a solvent-  
20 exposure of the Trp [40]. The evidence that Cys<sup>129</sup> is located in the vicinity of Trp<sup>135</sup> (see  
21 below: Figure 6A, B) together with the observation of the pronounced red shift of  $\lambda_{em-max}$   
22 compared to the wild type under reducing and oxidising conditions suggests a strong  
23 quenching effect of Cys<sup>129</sup> on Trp<sup>135</sup>-fluorescence. In conclusion a major conformational  
24 change takes place during the transition from the reduced to the oxidised state, whereby the  
25 formation of the disulfide bond between Cys54 and Cys171 is likely to play a significant role.

26

27 *The Significance of the Cysteinyll Residues for the Isomerisation Activity of CYP20-3.* CYP20-  
28 3 promotes the isomerisation of peptidyl prolyl residues from the *cis*- to the *trans*-form. To  
29 investigate the requirement of the conserved cysteinyll residues for the isomerisation activity,  
30 wild type CYP20-3 and the different Cys variants were analysed for PPI activity. The  
31 catalytic efficiency as expressed by  $k_{cat}/K_m$ -ratio is derived from the slope of the  
32 concentration-dependent  $k_{obs}$  values of the corresponding protein. They were determined  
33 under reducing and oxidising conditions, respectively (Figure 3, Table 2). The  $k_{cat}/K_m$ -ratio  
34 was  $4.23 \times 10^5 \text{ M}^{-1}\text{s}^{-1}$  for the reduced form and  $1.12 \times 10^5 \text{ M}^{-1}\text{s}^{-1}$  for the oxidised form of wild

1 type CYP20-3 (Figure 3, Table 2) confirming previous reports of oxidation-induced  
2 inactivation [31]. Elimination of three out of the four cysteinyl residues decreased the  
3 maximum catalytic PPI activity of the reduced CYP20-3. Activity remained unaltered in the  
4 case of CYP20-3<sub>C176S</sub> (CYP20-3<sub>C176S</sub>: kcat/Km =  $3.97 \times 10^5 \text{ M}^{-1}\text{s}^{-1}$ ) (Figure 3, Table 2). Under  
5 reducing conditions the mutation of Cys<sup>54</sup>, Cys<sup>129</sup> and Cys<sup>171</sup> into serine decreased the PPI  
6 activity by 60 %, 51 % and 75 % compared to the wild type, respectively. The isomerisation  
7 activities of the oxidised forms of CYP20-3<sub>C54S</sub>, CYP20-3<sub>C129S</sub> and CYP20-3<sub>C171S</sub> showed no  
8 significant differences compared to CYP20-3<sub>WT</sub>, whereas a significantly higher activity was  
9 observed for CYP20-3<sub>C171S</sub> (Figure 3, Table 2). Moreover, simultaneous mutation of Arg<sup>69</sup>  
10 and Phe<sup>74</sup>, which are essential amino acids for PPI activity and part of the so called RWFH-  
11 motif [3], into Ala<sup>69</sup> and Leu<sup>74</sup> respectively, abolished the PPI activity (data not shown).

12  
13 *The Midpoint Redox Potential of CYP20-3<sub>WT</sub> is -319 mV.* The midpoint redox potential of  
14 CYP20-3<sub>WT</sub> and the variants was determined using a fluorimetric test. The proteins were  
15 incubated in redox buffers adjusted with defined ratios of oxidised to reduced DTT, followed  
16 by labelling with excess monobromobimane (Figure 4). The wild type CYP20-3 midpoint  
17 redox potential was determined as  $-319 \pm 2 \text{ mV}$ . The midpoint redox potentials of the Cys  
18 mutants were more negative compared to the wild type, but only CYP20-3<sub>C176S</sub> showed a  
19 significant decrease (CYP20-3<sub>C54S</sub>:  $-320 \pm 4 \text{ mV}$ , CYP20-3<sub>C129S</sub>:  $-326 \pm 6 \text{ mV}$ , CYP20-3<sub>C171S</sub>:  
20  $-322 \pm 4 \text{ mV}$  and CYP20-3<sub>C176S</sub>:  $-327 \pm 3 \text{ mV}$ ; Figure 4).

21  
22 *The Cysteinyl Residues 129 and 171 of CYP20-3 are Required for the Regeneration of 2-Cys*  
23 *PrxA and 2-Cys PrxB.* Recently, Bernier-Villamor et al. [21] showed that the CYP20-3  
24 homologue from *Pisum sativum* is able to enhance the protective activity of 2-Cys Prx in a  
25 DNA protection assay. The chloroplasts of *Arabidopsis thaliana* contain four peroxiredoxins,  
26 namely 2-Cys PrxA and B, PrxQ and PrxII E [41]. To address the question whether  
27 *Arabidopsis* CYP20-3 is able to specifically reduce Prx the DNA protection assay in the  
28 presence of DTT/Fe<sup>3+</sup> was employed with different combinations of CYP20-3 and Prx. In a  
29 first set of experiments CYP20-3<sub>WT</sub> and the different CYP20-3 variants were tested for their  
30 ability to protect the plasmid-DNA either directly or by interaction with Prx. Neither reduced  
31 nor oxidized CYP20-3<sub>WT</sub> was able to protect the plasmid DNA (Figure 5A). Likewise, the  
32 CYP20-3 variants also showed no protection of DNA (Figure 5B). In a converse manner,  
33 CYP20-3<sub>WT</sub> increased the protective activity in the presence of 2-Cys PrxA (Figure 5C) and

1 2-Cys PrxB (Figure 5D). However, no reducing interaction was observed between CYP20-  
2 3<sub>WT</sub> and PrxQ (Figure 5E) or PrxII E (Figure 5F). To prove the functionality of the assay, the  
3 DNA protection was tested with known regenerators of PrxQ and 2-Cys PrxB. The results  
4 confirmed that 2-Cys Prx is regenerated by *E. coli* Trx [33], and PrxQ by the *A. thaliana* Trx  
5 y<sub>2</sub> [35], respectively, whereas no regenerator for PrxII E was found yet (Figure 5). On a  
6 comparative basis, the regeneration of 2-Cys PrxB was more efficient with Trx than with  
7 CYP20-3<sub>WT</sub> (Figure 5D). Until now, the mechanism of the CYP20-3/2-Cys Prx interaction is  
8 still not clarified. To identify the cysteines responsible for the reduction of 2-Cys PrxA and 2-  
9 Cys PrxB, the different CYP20-3 variants were tested. The addition of the variants CYP20-  
10 3<sub>C54S</sub> and CYP20-3<sub>C176S</sub> enhanced the fraction of supercoiled DNA and thus showed a better  
11 protective activity than the wild type. The other two cysteinyl variants had a similar protective  
12 pattern compared to the wild type (Figure 5C, 5D). In conclusion the cysteinyl residues Cys<sup>129</sup>  
13 and Cys<sup>171</sup> are most important for the interaction with 2-Cys PrxA and B. Interestingly, the  
14 CYP20-3<sub>ΔPPI</sub> variant showed a greater reducing activity than the wild type protein indicated  
15 by the lowest level of plasmid-DNA cleavage (Figure 5C, D).

## Discussion

16 *CYP20-3 Undergoes Major Conformational Changes in Dependence on Redox State.* CYP20-  
17 3<sub>WT</sub> shows altered electrophoretic mobility during the transition from the reduced to the  
18 oxidised form when separated under non-reducing conditions in the SDS-PAGE (Figure 1A).  
19 Motohashi et al. [31] have shown by 5,5'-dithio-bis(2-nitrobenzoic acid) labelling and  
20 MALDI-TOF mass spectrometry that oxidised CYP20-3 contains two redox-sensitive  
21 disulfide bonds, namely Cys<sup>54</sup>-Cys<sup>171</sup> and Cys<sup>129</sup>-Cys<sup>176</sup>, respectively. The formation of the  
22 disulfide bonds Cys<sup>54</sup>-Cys<sup>171</sup> and Cys<sup>129</sup>-Cys<sup>176</sup> [31] and the two observed redox-states of the  
23 CYP20-3<sub>WT</sub> protein (Figure 1A) indicate redox-dependent conformational changes as a basic  
24 mechanism for regulating CYP20-3 function. The electrophoretic mobility assays and the  
25 intrinsic fluorescence determinations (Figure 2, Table 1) revealed that the transition from the  
26 reduced to the oxidised state of CYP20-3 as well as the stability of the oxidised form depend  
27 on the formation of both disulfide bonds. In addition, the results from intrinsic fluorescence  
28 analysis (Figure 2, Table 1) assign a predominant role in conformational dynamics to the  
29 disulfide bridge formation between Cys<sup>54</sup> and Cys<sup>171</sup>. The intrinsic fluorescence analysis also  
30 confirms that Cys<sup>54</sup> and Cys<sup>171</sup>, and Cys<sup>129</sup> and Cys<sup>176</sup> cooperate in disulfide bond formation

1 [31] since the corresponding variants revealed identical alterations.

2

3 *Cysteinyln Residues Affect CYP20-3 Isomerisation Activity.* CYP20-3 promotes the  
4 isomerisation of prolyl bonds from the *cis*- to the *trans*-form. This study provides answers to  
5 two redox-related questions, namely: (i) does the isomerisation activity depend on the thiol  
6 redox state, and (ii) are all cysteinyln residues equally important in respect to the PPI activity.  
7 In accordance with previous reports [31] the isomerisation activity of CYP20-3<sub>WT</sub> was  
8 modulated by the redox milieu being less active under oxidising conditions when disulfide  
9 bonds between Cys<sup>54</sup> and Cys<sup>171</sup> as well as Cys<sup>129</sup> and Cys<sup>176</sup> are formed (Figure 3, Table 2).  
10 The *k*<sub>cat</sub>/*K*<sub>m</sub>-value for reduced CYP20-3<sub>WT</sub> ( $4.23 \times 10^5 \text{ M}^{-1}\text{s}^{-1}$ ) was 6- to 40-fold lower than  
11 previously reported for CYP20-3<sub>WT</sub> of *A. thaliana* ( $8.2 \times 10^6 \text{ M}^{-1}\text{s}^{-1}$ ; [31]), CeCyp3 (*k*<sub>cat</sub>/*K*<sub>m</sub>:  
12  $2.4 \times 10^6 \text{ M}^{-1}\text{s}^{-1}$ ; [42]) or human HsCypA ( $1.4 \times 10^7 \text{ M}^{-1}\text{s}^{-1}$ ; [37]). All mutations caused  
13 changes regarding the isomerisation activity under reducing and oxidising conditions  
14 compared to CYP20-3<sub>WT</sub>. This implies alterations in the chemical vicinity of the RWFH-motif  
15 in the variants. The low catalytic efficiency observed in the apparently reduced CYP20-3<sub>C171S</sub>  
16 variant (Figures 1D and 3D, Table 2) supports the conclusion that Cys<sup>171</sup> is most important to  
17 maintain maximum PPI activity. The wild type-like catalytic activity of reduced CYP20-  
18 3<sub>C176S</sub> on the other hand indicates a minor role in PPI activity, but a major role in oxidative  
19 inactivation since CYP20-3<sub>C176S</sub> maintained a very high catalytic efficiency. The thiol-  
20 dependency of CYP20-3 PPI activity contrasts the insensitivity of human CypA (HsCypA)  
21 PPI to mutation of the cysteinyln residues 52, 62, 115 and 161 [37] although two of the four  
22 Cys-residues of HsCypA are located within the PPI-motif. Interestingly only Cys<sup>129</sup> and  
23 Cys<sup>176</sup> are conserved among plant and human Cyp, whereas Cys<sup>54</sup> and Cys<sup>171</sup> in the plant  
24 protein is absent from the human protein (Fig. 6B). Accordingly, the disulfide bridge between  
25 Cys<sup>54</sup> and Cys<sup>171</sup> is essential for the redox control of the PPI activity.

26

27 *Importance of the Disulfide Bonds.* The midpoint redox potential of CYP20-3<sub>WT</sub> was  
28 determined to be  $-319 \pm 2 \text{ mV}$  (Figure 4, Table 3). The midpoint redox potentials of the  
29 variants were similar to that of the wild type. It may be postulated that the oxidation of one  
30 disulfide bond alters the redox potential of the second disulfide bond causing a easier/faster  
31 oxidation. However, it was impossible to determine the midpoint redox potentials for each  
32 disulfide bond independently. The variants CYP20-3<sub>C54S</sub> (320 mV) and CYP20-3<sub>C171S</sub> (322  
33 mV) have a slightly less negative redox potential than the other two variants (CYP20-3<sub>C129S</sub>:

1 326 mV and CYP20-3<sub>C176S</sub>: 326 mV). In the variants CYP20-3<sub>C54S</sub> and CYP20-3<sub>C171S</sub> the  
2 midpoint redox potential of the disulfide bridge between Cys<sup>129</sup> and Cys<sup>176</sup> is less negative  
3 indicating an easier reduction. In a converse manner, the disulfide bridge between Cys<sup>54</sup> and  
4 Cys<sup>171</sup> is more easily formed than the disulfide bridge between Cys<sup>129</sup> and Cys<sup>176</sup>. This  
5 interpretation is still speculative in the light of the similarity and the standard deviation of the  
6 determined redox midpoint potentials. But this hypothesis fits into the emerging picture that  
7 the disulfide bond between Cys<sup>54</sup> and Cys<sup>171</sup> is the more important one for the redox  
8 properties of functional CYP20-3. These two cysteinyl residues are conserved in other  
9 *Arabidopsis* cyclophilins. It will have to be tested whether these proteins also are regulated by  
10 thiol/disulfide transition. On the other hand, amino acids corresponding to Cys<sup>176</sup> lack in all  
11 other members of the *Arabidopsis* cyclophilin protein family [3].

12  
13 *CYP20-3 as Regenerator of Chloroplast Peroxiredoxins.* With -319 was the midpoint redox  
14 potential of CYP20-3<sub>WT</sub> more negative than that of 2-Cys Prx A with an Em of -307 mV [33].  
15 Reductive activation of CYP20-3 is likely to occur under conditions of excess electron  
16 pressure in photosynthesis. In accordance to other publications, *in vitro* experiments revealed  
17 Trx-m as an interaction partner of CYP20-3: Trx-m with an Em of -300 mV is able to reduce  
18 CYP20-3 and to activate its PPI activity [30; 31; 43]. Recently, Lee et al. [20] reported that  
19 HsCypA activates human peroxiredoxins and Bernier-Villamor et al. [21] showed that a  
20 CYP20-3-homologue from *Pisum sativum* supports the peroxide-detoxifying activity of plant  
21 2-Cys Prx. The midpoint redox potentials of chloroplast Prxs range between -290 mV for  
22 PrxII E, -307 mV for 2-Cys Prx A, -322 mV for 2-Cys Prx B and -325 mV for PrxQ [22;  
23 44]. Thus based on redox potentials, all chloroplast Prxs are potential targets for CYP20-3,  
24 considering that an efficient reduction of the regulatory disulfides still can occur in the  
25 presence of a  $\Delta E_m$  of up to 20 mV [44]. The DNA-protection assay manifested the ability of  
26 CYP20-3 to reduce 2-Cys PrxA and 2-Cys PrxB (Figure 5) similar to *E. coli* Trx [33] and  
27 *Arabidopsis* Trx-m, -y1, -y2 and -x [35]. In a converse manner the combination of PrxII E  
28 and PrxQ, respectively, in combination with CYP20-3 gave no protection of plasmid-DNA in  
29 the DNA-cleavage assay (Figure 5E, F). It is concluded that CYP20-3 is unable to efficiently  
30 reduce PrxQ and PrxII E. This suggests that 2-Cys PrxA and 2-Cys PrxB are specific  
31 interaction partners of CYP20-3 at least *in vitro*.

32 The redox-dependent properties of cyclophilins may also be relevant in other organisms.  
33 *Caenorhabditis elegans* Cyp3 (CeCyp3) that shows a similarity at the protein primary

1 sequence level of 63% to CYP20-3 possesses four cysteine residues at conserved positions  
2 homologous to the four in CYP20-3 suggesting similar function (Figure 6B) [42]. The authors  
3 proposed that CeCyp3 might play a role in a signalling response to oxidative stress.

4 The DNA-cleavage assay proved Prx-reducing activity of all four variants, but the particular  
5 importance of Cys<sup>129</sup> and Cys<sup>171</sup> in the reduction of 2-Cys PrxA and 2-Cys PrxB (Figure 5C,  
6 D). Lee et al. [20] found Cys<sup>115</sup> and Cys<sup>161</sup> of human CypA corresponding to Cys<sup>129</sup> and  
7 Cys<sup>176</sup> of CYP20-3 (Figure 6B) to be important for the reduction of human Prx II using the  
8 glutamine synthetase protection assay. Taking together the results of the PPI activity  
9 measurements (Figure 3) and the DNA-protection assay (Figure 5) suggest that Cys<sup>171</sup> is  
10 involved in both redox-related functions. The CYP20-3<sub>ΔPPI</sub> variant showed an increased  
11 reducing activity towards 2-Cys PrxA and 2-Cys PrxB (Figure 5C, D) implicating that Cys<sup>129</sup>  
12 or Cys<sup>171</sup> is better accessible for oxidised 2-Cys PrxA and 2-Cys PrxB after changing the  
13 thiols in close vicinity of the active centre. As the CYP20-3<sub>ΔPPI</sub> variant showed no  
14 isomerisation activity (data not shown), but greater reducing activity, it can be concluded that  
15 both functions of CYP20-3, i.e. the catalytic activity as PPIase and the function as reductant,  
16 are independent from each other. Nevertheless both functions are regulated in dependence on  
17 the redox status of the active centre of CYP20-3. The best-known mechanism to modify  
18 cyclophilin activity is the binding of cyclosporin A (CsA), an immunosuppressive drug that  
19 specifically inhibits the cyclophilin PPIase activity [4]. Subsequently, the CsA-Cyp complex  
20 binds to subunit B of the Ca<sup>2+</sup>/calmodulin-dependent Ser-/Thr-phosphatase calcineurin  
21 leading to its inactivation and, finally, resulting in altered gene transcription in the nucleus  
22 [45; 46]. Thus, the electron donating property of CYP20-3 to 2-Cys Prx as observed in the  
23 DNA-protection assay not necessarily indicates a major role of CYP20-3 in the antioxidant  
24 defence of the chloroplast but a role in the redox signalling network adjusting the redox state  
25 and thereby the activity of CYP20-3. In this scenario, the 2-Cys Prx serves as peroxide sensor  
26 transmitting redox information to CYP20-3 that in turn modulates target protein functions  
27 [47]. It will be necessary to identify other interacting partners and thus regulatory targets of  
28 CYP20-3. Furthermore, the analysis of *Arabidopsis* lines lacking or overexpressing CYP20-3  
29 protein will possibly allow clarifying its physiological role within the plant redox network in  
30 the adaptation process to stress.

**Acknowledgements:**

Expert technical assistance by Heike Bogunovic is gratefully acknowledged. Trx y1 was kindly provided by Dr. Emmanuelle Issakidis-Bourguet and Dr. Myroslawa Miginiac-Maslow. We thank Dr. Andreas Brockhinke for helpful discussion. Research was supported by Bielefeld University within the FIF-initiative and by the Deutsche Forschungsgemeinschaft within the SFB 613 (D9), but also FOR 387 (TP3).

**References:**

- 1 He, Z., Li, L. and Luan S. (2004) Immunophilins and parvulins. Superfamily of peptidyl prolyl isomerases in Arabidopsis. *Plant Physiol.* **134**, 1248-1267
- 2 Buchanan, B. B. and Luan, S. (2005) Redox regulation in the chloroplast thylakoid lumen: a new frontier in photosynthesis research. *J. Exp. Bot.* **56**, 1439-1447
- 3 Romano, P. G. N., Horton, P. and Gray J. E. (2004) The Arabidopsis cyclophilin gene family. *Plant Physiol.* **134**, 1268-1282
- 4 Handschumacher, R. E., Harding, M. W., Rice, J. and Drugge, R.J. (1984) Cyclophilin: A specific cytosolic binding protein for cyclosporin A. *Science* **226**, 544-547
- 5 Romano, P. G. N., Gray, J., Horton, P. and Luan S. (2005) Plant immunophilins: functional versatility beyond protein maturation. *New Phytol.* **166**, 753-769
- 6 Bächinger, H. P. (1987) The influence of peptidyl-prolyl *cis-trans* isomerase on the in vitro folding of type III collagen. *J. Biol. Chem.* **262**, 17144-17148
- 7 Davis, J. M., Boswell, B. A. and Bächinger, H. P. (1989) Thermal stability and folding of type IV procollagen and effect of peptidyl-prolyl *cis-trans*-isomerase on the folding of the triple helix. *J. Biol. Chem.* **264**, 8956-8962
- 8 Schönbrunner, E. R. and Schmid, F. X. (1992) Peptidyl-prolyl *cis-trans* isomerases improve the efficiency of protein disulfide isomerase as a catalyst of protein folding. *Proc. Natl. Acad. Sci. U.S.A.* **89**, 4510-4513
- 9 Gupta, R., Mould, R. M., He, Z. and Luan, S. (2002) A chloroplast FKBP interacts with and affects the accumulation of Rieske subunit of cytochrome bf complex. *Proc. Natl. Acad. Sci. U.S.A.* **99**, 15806-15811
- 10 Freskgard, P. O., Bergenheim, N., Johnsson, B. H., Svensson, M. and Carlsson, U. (1992) Isomerase and chaperone activity of prolyl isomerase in the folding of carbonic anhydrase. *Science* **258**, 466-468

- 11 Freeman, B. C., Toft, D. O. and Morimoto R. I. (1996) Molecular chaperone machines: chaperone activities of the Cyp-40 and the steroid aporeceptor associated protein p23. *Science* **274**, 1718-1720
- 12 Maleszka, R., Lupas, A., Hanes, S. D. and Miklos, G. L. (1997) The dodo gene family encodes a novel protein involved in signal transduction and protein folding. *Gene* **203**, 89-93
- 13 Brazin, K. N., Mallis, R. J., Fulton, D. B. and Andreotti, A. H. (2001) Regulation of the tyrosine kinase Itk by the peptidyl-prolyl isomerase cyclophilin A. *Proc. Natl. Acad. Sci. U.S.A.* **99**, 1899-1904
- 14 Jin, Z.-G., Melaragno, M. G., Liao, D.-F., Yan, C., Haendeler, J., Suh, Y.-A, Lambeth, J. D., Berk, B. C. (2000) Cyclophilin A is a secreted growth factor induced by oxidative stress. *Circ. Res.* **87**, 789-796
- 15 Luan S., Lane W. S. and Schreiber S. L. (1994) pCyp B: a chloroplast-localized, heat shock-responsive cyclophilin from fava bean. *Plant Cell* **6**, 885-892
- 16 Meza-Zepeda, L. A., Baudo, M. M., Palva, E. T. and Heino P. (1998) Isolation and characterization of a cDNA corresponding to a stress-activated cyclophilin gene in *Solanum commersonii*. *J. Exp. Bot.* **49**, 1451-1452
- 17 Berardini, T. Z., Bollmann, K., Sun, H. and Poethig, R. S. (2001) Regulation of vegetative phase change in *Arabidopsis thaliana* by cyclophilin 40. *Science* **291**, 2405-2407
- 18 Horowitz, D. S., Lee, E. J., Mabon, S. A. and Misteli, T. (2002) A cyclophilin function in pre-mRNA splicing. *EMBO J.* **21**, 470-480
- 19 Ingelfinger, D., Göthel, S. F., Marahiel, M. A., Reidt, U., Ficner, R., Lührmann, R. and Achsel, T. (2003) Two protein-protein interaction sites on the spliceosome-associated human cyclophilin CypH. *Nucleic Acids Res.* **31**, 4791-4796
- 20 Lee, S. P., Hwang, Y. S., Kim, Y. J., Kwon, K.-S., Kim, H. J., Kim, K. and Chae, H. Z. (2001) Cyclophilin A binds to peroxiredoxins and activates its peroxidase activity. *J. Biol. Chem.* **276**, 29826-29832
- 21 Bernier-Villamor, L., Navarro, E., Sevilla, F. and Lázaro, J.-J. (2004) Cloning and characterization of a 2-Cys peroxiredoxin from *Pisum sativum*. *J. Exp. Bot.* **55**, 2191-2199
- 22 Horling, F., Lamkemeyer, P., König, J., Finkemeier, I., Kandlbinder, A., Baier, M. and Dietz, K.-J. (2003) Divergent light-, ascorbate-, and oxidative stress-dependent

- regulation of expression of the peroxiredoxin gene family in *Arabidopsis*. *Plant Physiol.* **131**, 317-325
- 23 Hofmann, B., Hecht, H. J. and Flohe L. (2002) Peroxiredoxins. *J. Biol. Chem.* **383**, 347-364
- 24 König, J., Lotte, K., Plessow, R., Brockhinke, A., Baier, M. and Dietz, K.-J. (2003) Reaction mechanism of plant 2-Cys peroxiredoxin: role of the C-terminus and the quaternary structure. *J. Biol. Chem.* **278**, 24409-24420
- 25 Dietz, K.-J. (2003) Plant peroxiredoxins. *Ann. Rev. Plant Biol.* **54**, 93-107
- 26 Dietz, K.-J., Jacob, S., Oelze, M.-L., Laxa, M., Tognetti, V., de Miranda, S.M., Baier, M. and Finkemeier, I. (2006) The function of peroxiredoxins in plant organelle redox metabolism. *J. Exp. Bot.* **57**, 1697-1709
- 27 Finkemeier, I., Goodman, M., Lamkemeyer, P., Kandlbinder, A., Sweetlove, L. J. and Dietz K.-J. (2005) The mitochondrial type II peroxiredoxin F is essential for redox homeostasis and root growth of *Arabidopsis thaliana* under stress. *J. Biol. Chem.* **280**, 12168-12180
- 28 Lippuner, V., Chou, I. T., Scott, S. V., Ettinger, W. F., Theg, S. M. and Gasser C. S. (1994) Cloning and characterization of chloroplast and cytosolic forms of cyclophilin from *Arabidopsis thaliana*. *J. Biol. Chem.* **269**, 7863-7868
- 29 Schubert, M., Petersson, U. A., Haas, B. J., Funk, C., Schröder, W. P. and Kieselbach, T. (2002) Proteome map of the chloroplast lumen of *Arabidopsis thaliana*. *J. Biol. Chem.* **277**, 8354-8365
- 30 Motohashi, K., Kondoh, A., Stumpp, M. T. and Hisabori T. (2001) Comprehensive survey of proteins targeted by chloroplast thioredoxin. *Proc. Natl. Acad. Sci. U.S.A.* **98**, 11224-11229
- 31 Motohashi, K., Koyama, F., Nakanishi, Y., Ueoka-Nakanishi, H. and Hisabori, T. (2003) Chloroplast cyclophilin is a target protein of thioredoxin. *J. Biol. Chem.* **278**, 31848-31852
- 32 Montemartini, M., Kalisz, H. M., Hecht, H. J., Steinert, P. and Flohe, L. (1999) Activation of active-site cysteine residues in the peroxiredoxin-type trypanoxin peroxidase of *Crithidia fasciculata*. *Eur. J. Biochem.* **264**, 516-524
- 33 König, J., Baier, M., Horling, F., Kahmann, U., Harris, G., Schürmann, P. and Dietz, K.-J. (2002) The plant-specific function of 2-Cys peroxiredoxin-mediated detoxification of peroxides in the redox-hierarchy of photosynthetic electron flux. *Proc. Natl. Acad. Sci. U.S.A.* **99**, 5738-5743

- 34 Yamamoto, H., Miyake, C., Dietz, K.-J., Tomizawa, K. I., Murata, N. and Yokota, A. (1999) Thioredoxin peroxidase in the cyanobacterium *Synechocystis* sp. PCC 6803. *FEBS Lett.* **447**, 269-273
- 35 Collin, V., Lamkemeyer, P., Miginiac-Maslow, M., Hirasawa, M., Knaff, B. D., Dietz, K.-J. and Issakidis-Bourguet, E. (2004) Characterization of plastidial thioredoxins from *Arabidopsis* belonging to the new y-type1. *Plant Physiol.* **136**, 4088-4095
- 36 Fischer, G., Bang, H., Berger, E. and Schellenberger A. (1984) Conformational specificity of chymotrypsin toward proline-containing substrates. *Biochim. Biophys. Acta* **791**, 87-97
- 37 Liu, J., Albers, M. W., Chen, C.-M., Schreiber, S. L. and Walsh, C. T. (1990) Cloning, expression, and purification of human cyclophilin in *Escherichia coli* and assessment of the catalytic role of cysteines by site-directed mutagenesis. *Proc. Natl. Acad. Sci. U.S.A.* **87**, 2304-2308
- 38 Hirasawa, M., Schürmann, P., Jacquot, J.-P., Manieri, W., Jacquot, P., Keryer, E., Hartman, F.C. and Knaff, D.B. (1999) Oxidation-reduction properties of chloroplast thioredoxins, ferredoxin: thioredoxin reductase, and thioredoxin f-regulated enzymes. *Biochemistry* **38**, 5200-5205
- 39 Teale, F. W. J. and Weber, G. (1957) Ultraviolet fluorescence of the aromatic amino acids. *Biochem. J.* **65**, 476-482
- 40 Burstein, E. A., Vedenkins, N. S. and Ivkova, M. N. (1973) Fluorescence and the location of tryptophan residues in protein molecules. *Photochem. Photobiol.* **18**, 263-279
- 41 Dietz, K.-J., Horling, F., König, J. and Baier, M. (2002) The function of the chloroplast 2-cysteine peroxiredoxin in peroxide detoxification and its regulation. *J. Exp. Bot.* **53**, 1321-1329
- 42 Dornan, J., Page, A. P., Taylor, P., Wu, S.-Y., Winter, A. D., Husi, H. and Walkinshaw, M. D. (1999) Biochemical and structural characterization of a divergent loop cyclophilin from *Caenorhabditis elegans*. *J. Biol. Chem.* **274**, 34877-34883
- 43 Hisabori, T., Hara, S., Fujii, T., Yamazaki, D., Hosoya-Matsuda, N. and Motohashi, K. (2005) Thioredoxin affinity chromatography: a useful method for further understanding the thioredoxin network. *J. Exp. Bot.* **56**, 1463-1468
- 44 Rouhier, N., Gelhaye, E., Gualberto, J. M., Jordy, M.-N., De Faye, E., Hirasawa, M., Duplessis, S., Lemaire, S. D., Frey, P., Martin, F., Manier, I. W., Knaff, D. B. and

- Jaquot J.-P. (2004) Poplar peroxiredoxin Q. A thioredoxin-linked antioxidant functional in pathogen defense. *Plant Physiol.* **134**, 1027-1038
- 45 Liu, J., Farmer, J. D., Lane, W. S., Friedman, J., Weissman, I. and Schreiber, S. L. (1991) Calcineurin is a common target of cyclophilin-cyclosporin A and FKBP-FK506 complexes. *Cell* **66**, 807-815
- 46 Li, W. and Handschumacher, R. E. (1993) Specific interaction of the cyclophilin-cyclosporin complex with the B subunit of calcineurin. *J. Biol. Chem.* **268**, 14040-14044
- 47 Dietz, KJ. (2003) Redox regulation, redox signalling and redox homeostasis in plant cells. *Intern. Rev. Cytol.* **228**:141-193.

**Legends to the figures and tables:**

1

**Figure 1: Protein mobility shift of the recombinant CYP20-3<sub>WT</sub> and Cys→Ser variants.**

2 0.5 µg Cyp was incubated with various concentrations of either H<sub>2</sub>O<sub>2</sub> or DTT at RT for 15  
3 min. All samples were analysed by SDS-16 % PAGE separation and subsequent silver  
4 staining (A-F).

6

**Figure 2: Intrinsic Trp fluorescence emission spectra of CYP20-3<sub>WT</sub> and the Cys → Ser variants as a function of thiol redox state.**

7 Trp fluorescence of the proteins was measured  
8 under reducing (black line) and oxidising (grey line) conditions after excitation at  $\lambda_{\text{ex}} = 290$   
9 nm ( $n \geq 9$  for each protein). Data were fitted with the software program FindGraph. The  
10 wavelengths of the emission maxima ( $\lambda_{\text{em-max}}$ ) are given in Table 1.

12

**Figure 3: Observed velocity,  $k_{\text{obs}}$ , with different concentrations of wild type CYP20-3 and the Cys → Ser variants under reducing or oxidising conditions.**

13 The PPI activity was  
14 assayed using N-succinyl-Ala-Ala-Pro-Phe-p-nitroanilide. Variation of the amount of enzyme  
15 led to a family of curves and generated the linear correlation of  $k_{\text{obs}}$  versus protein  
16 concentrations. As described in 'Material and Methods', the slope of each line equals  
17 kcat/Km for the corresponding protein either under reducing or oxidising conditions as listed  
18 in Table 2. Assay (A) wild type CYP20-3, (B) CYP20-3<sub>C54S</sub>, (C) CYP20-3<sub>C129S</sub>, (D) CYP20-  
19 3<sub>C171S</sub> and (E) CYP20-3<sub>C176S</sub> ( $n \geq 3 \pm \text{SD}$ ). Symbols, regression lines and error bars represent  
20 reducing and oxidising conditions as follows: o, — and black error bars: 10 mM DTT; ■, - - -  
21 and grey error bars: 10 mM H<sub>2</sub>O<sub>2</sub> ( $n \geq 3 \pm \text{SD}$ ).

23

**Figure 4: Titration of the midpoint redox potential of CYP20-3<sub>WT</sub> and the Cys → Ser variants.**

24 The redox potential of the samples was adjusted by varying the ratio of  
25  $\text{DTT}_{\text{oxidised}}/\text{DTT}_{\text{reduced}}$ . Reduced thiol groups were labelled with monobromobimane and the  
26 samples analysed for bound fluorophore. Experimental data were fitted to the Nernst equation  
27 with  $n = 4$  (wild type) or  $n = 3$  (variants) using GraFit5. Midpoint redox potentials ( $E_{\text{m}}$ ;  
28 means  $\pm \text{SD}$  of two or more experiments for each protein) are indicated in the figure.

30

31 **Figure 5: DNA protection assay as indicator of CYP20-3-dependent reduction of the**  
32 **chloroplastic peroxiredoxins.** In each experiment (1) represents the control without 3 µM  
33 FeCl<sub>3</sub>/10 mM DTT and (2) the maximum cleavage of the plasmid DNA achieved in that

1 particular experiment with 3  $\mu$ M FeCl<sub>3</sub>/10 mM DTT but without added protein. (A) Effect of  
2 CYP20-3 redox-state and cyclosporin A (CsA) on DNA cleavage in the absence of Prx. (B)  
3 Effect of CYP20-3 and the different Cys→ Ser variants (each 3  $\mu$ g) on DNA cleavage. (C)  
4 Effect of CYP20-3 and Cys→ Ser variants (each 3  $\mu$ g) on 2-Cys PrxA (6  $\mu$ g) -mediated DNA  
5 protection. (D) Effect of CYP20-3 and Cys→ Ser variants (each 3  $\mu$ g) on 2-Cys PrxB-  
6 mediated DNA protection. Thioredoxin was added as an efficient donor control. (E) Effect of  
7 CYP20-3 on PrxQ-dependent DNA protection (6  $\mu$ g). (F) Effect of CYP20-3 on PrxII E-  
8 dependent DNA protection. The percentage of open circular plasmid-DNA, indicating ROS-  
9 mediated cleavage, is given for each experiment. Each experiment was performed  $\geq$  3 times  
10 with similar results.

11

12 **Figure 6: (A) Localisation of the cysteinyl residues 54, 129, 171 and 176 as well as Trp**  
13 **135 in the tertiary structure and in comparison to the active centre represented by the**  
14 **R-F-W-H-motif of the CYP20-3 molecule.** The Cys54 and 176 are arranged very close  
15 together in the structure of CYP20-3 and are part of the surface of the molecule, therefore,  
16 possibly being accessible to reactive oxygen species (ROS). The Cys129 and 171 are located  
17 on the opposite site of the molecule compared to Cys54 and 176. The model was calculated  
18 based on known structures of human CypB and Cyp3 from *C. elegans*, respectively, using  
19 Deep View/Swiss-Pdb Viewer 3.7 ([www.expasy.org/spdbw/](http://www.expasy.org/spdbw/)) and further processed by using  
20 Rasmol. **(B) Amino acid sequence alignment of the *A. thaliana* cyclophilin CYP20-3**  
21 **(B53422, without the signal peptide of 77 amino acids), CypA from *H. sapiens* (P62937)**  
22 **and Cyp3 from *C. elegans* (NP\_506751).** The conserved cysteinyl residues are shaded and  
23 the catalytic motif of a typical PPI is underlined.

Laxa et al., 2006

**Table 1: Emission maximum wavelengths ( $\lambda_{em-max}$ ) for CYP20-3<sub>WT</sub> and the Cys→ Ser variants under reducing and oxidising conditions.** Data were fitted by an asymmetric Gaussian equation using the software program FindGraph and analysed for the wavelength of maximum emission. Also given are the calculated differences between the maximum wavelengths of variants minus wildtype under reducing (column 3) and oxidising conditions (column 5) and the difference between oxidising and reducing conditions (column 6).

	Reduced		Oxidised		Difference
	$\lambda_{em-max}$ [nm]	shift (variant-wt) [nm]	$\lambda_{em-max}$ [nm]	shift (variant-wt) [nm]	oxidized-reduced [nm]
CYP20-3 <sub>WT</sub>	339.2	± 0.0	337.6	± 0.0	- 1.6
CYP20-3 <sub>C54S</sub>	333.7	- 5.5	336.4	- 1.2	+ 2.7
CYP20-3 <sub>C129S</sub>	344.1	+ 4.9	344.9	+ 7.3	+ 0.8
CYP20-3 <sub>C171S</sub>	335.2	- 4.0	338.0	+ 0.4	+ 2.8
CYP20-3 <sub>C176S</sub>	334.4	- 4.8	334.1	- 3.5	- 0.3

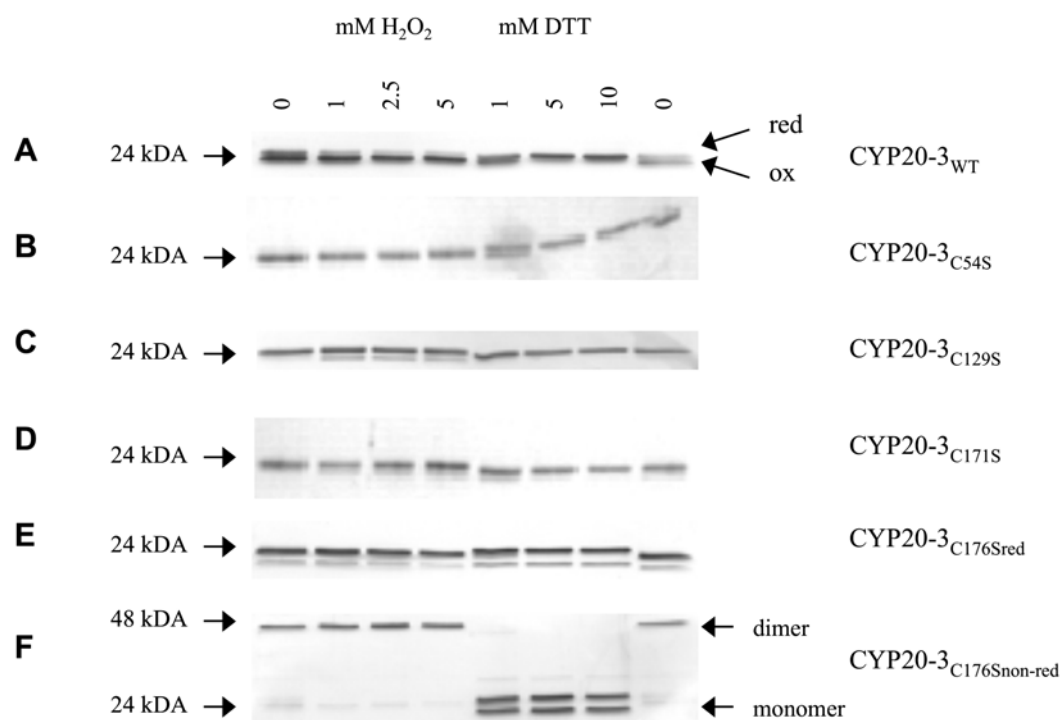
## Laxa et al., 2006

1 **Table 2: Kcat/Km-values [ $s^{-1} M^{-1}$ ] for the PPIs of CYP20-3<sub>WT</sub> and the Cys→ Ser**  
 2 **variants.** Various concentrations of Cyp were incubated with either 10 mM DTT or 10 mM  
 3 H<sub>2</sub>O<sub>2</sub>. Kcat/Km-values were determined as described in 'Materials and Methods'.  
 4

	Reduced		Oxidised	
	Kcat/Km-values [ $s^{-1} M^{-1}$ ]	[%]	Kcat/Km-values [ $s^{-1} M^{-1}$ ]	[%]
CYP20-3 <sub>WT</sub>	$4.23 \times 10^5$	100	$1.12 \times 10^5$	100
CYP20-3 <sub>C54S</sub>	$1.71 \times 10^5$	40.4	$1.38 \times 10^5$	123.2
CYP20-3 <sub>C129S</sub>	$2.06 \times 10^5$	48.7	$0.94 \times 10^5$	83.9
CYP20-3 <sub>C171S</sub>	$1.06 \times 10^5$	25.1	$0.97 \times 10^5$	86.6
CYP20-3 <sub>C176S</sub>	$3.97 \times 10^5$	93.9	$2.59 \times 10^5$	231.3

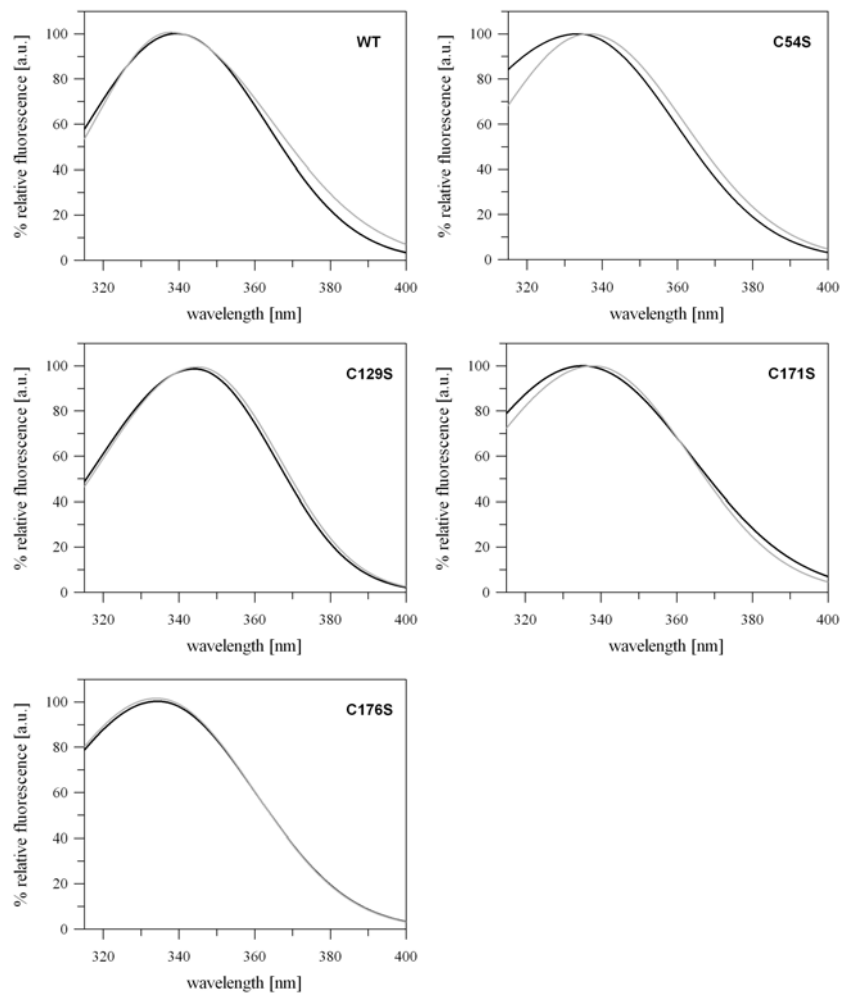
**Laxa et al., 2006**

**Figure 1:**



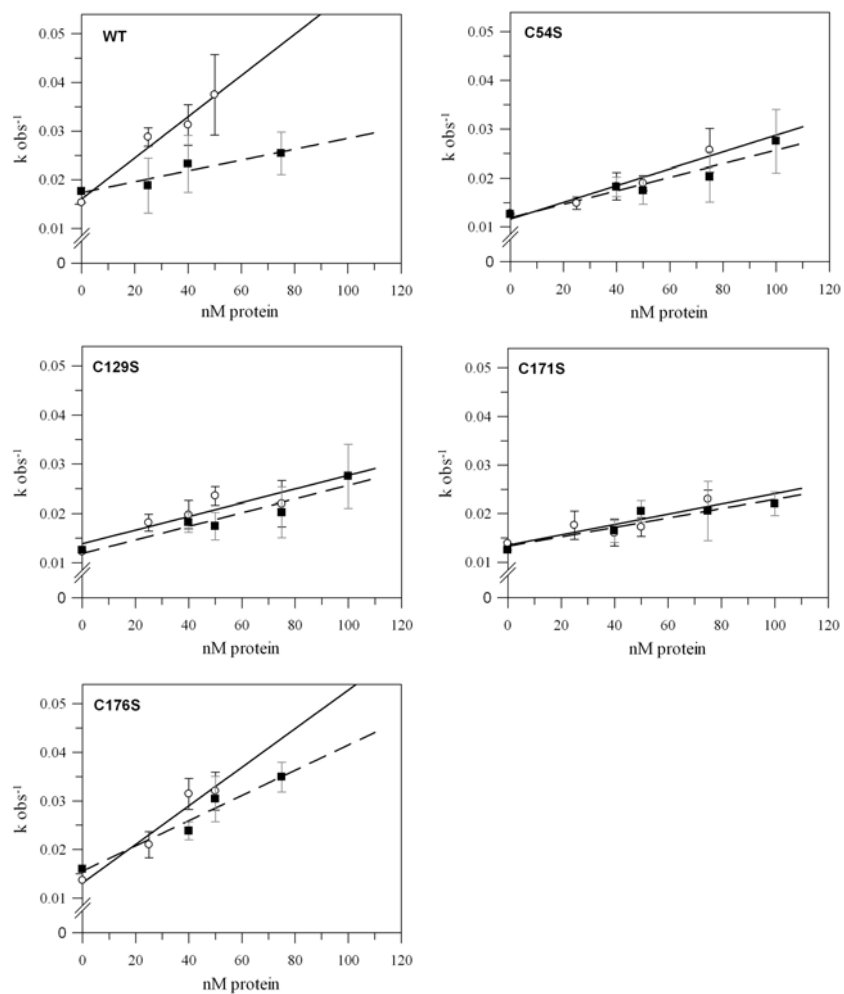
Laxa et al., 2006

Figure 2:



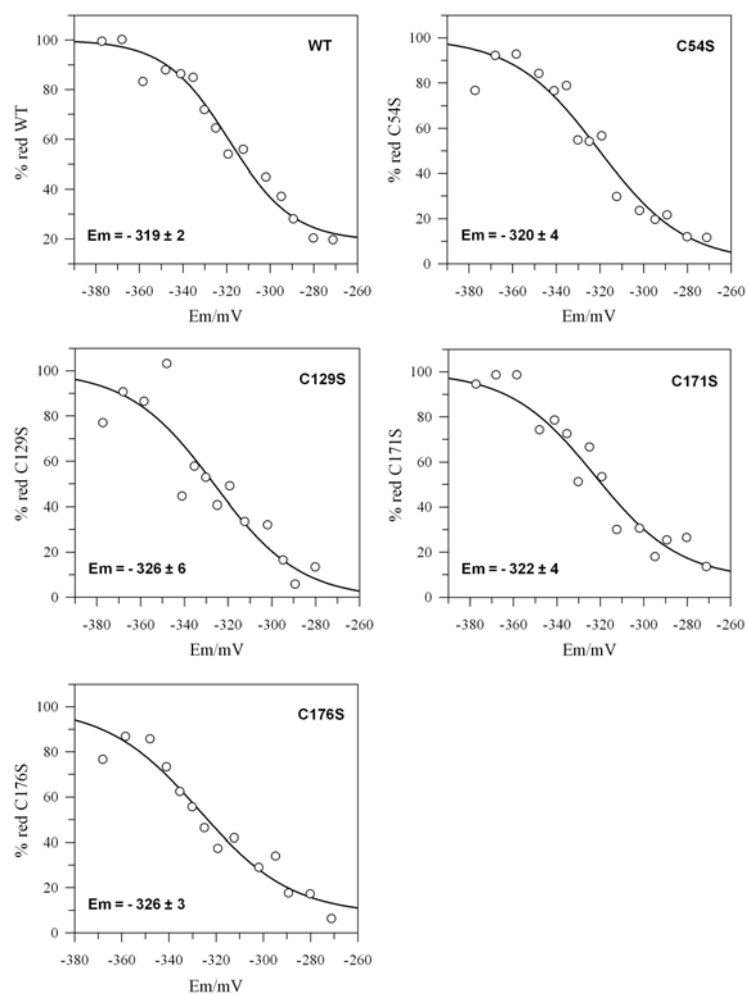
Laxa et al., 2006

Figure 3:



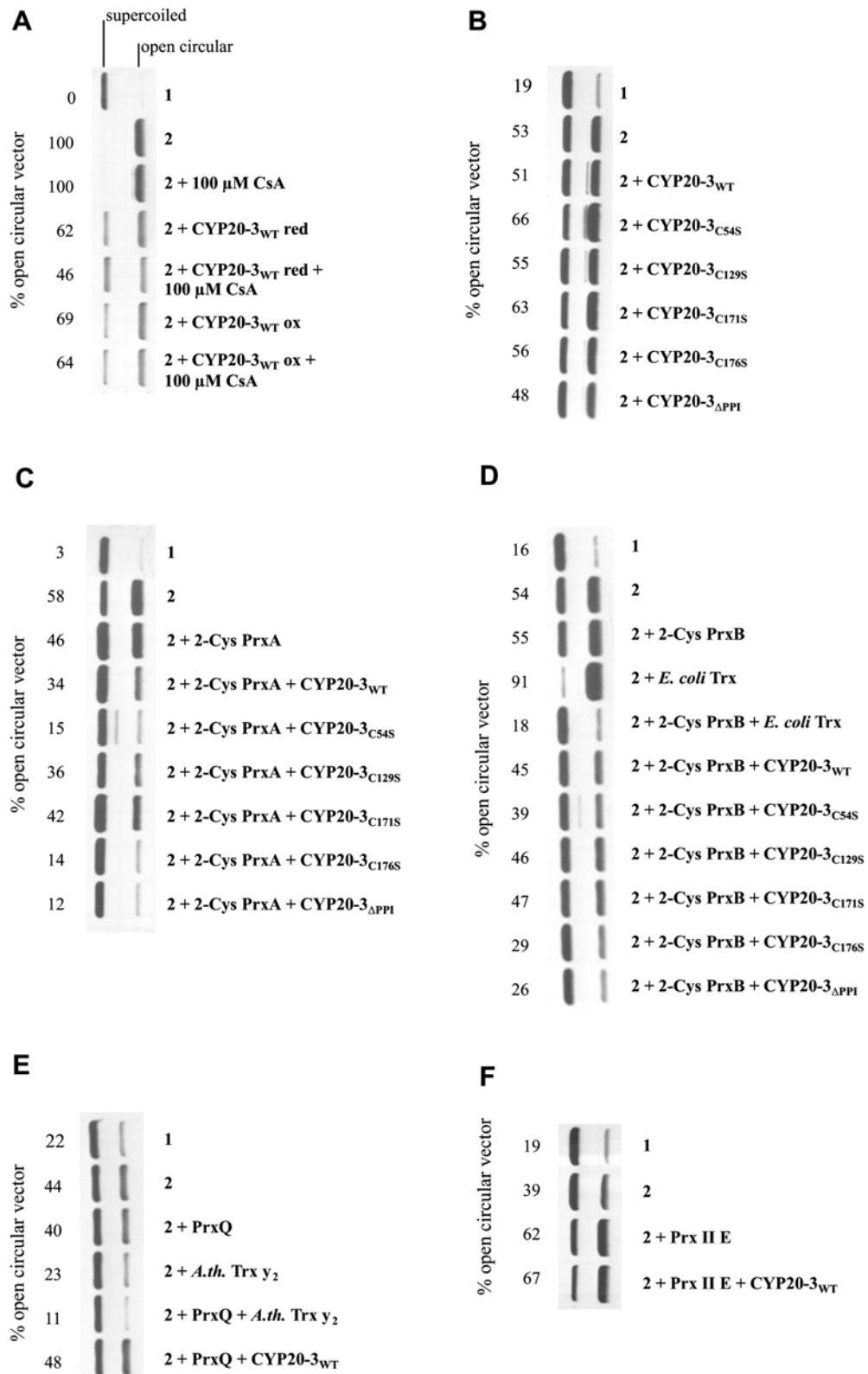
Laxa et al., 2006

Figure 4:



Laxa et al., 2006

Figure 5:



Laxa et al., 2006

Figure 6A:

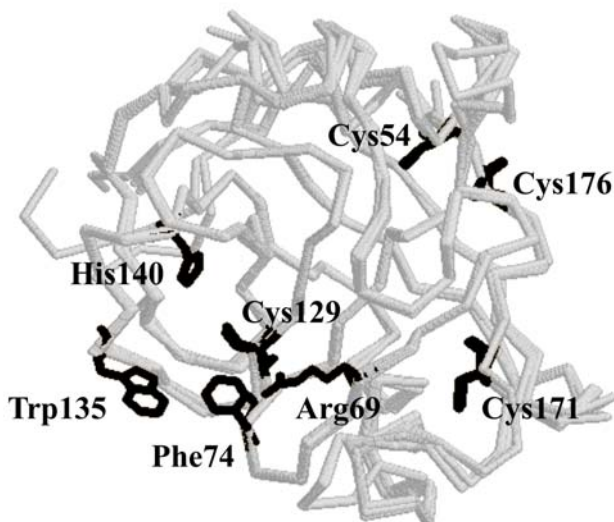


Figure 6B:

```

HsCypA -----
CeCyp3 -----
AtCyp20-3 MASSSSMQMVHTSRSlAQlGfGVKSQlVlSANRtTQSVCFGARSSGIALSSRLHYASPIKQ 60

HsCypA -----MVNPTVFFDlAVDGEPLGRVlSFELFADKV 29
CeCyp3 -----MSRSKVFFDlTlGGKASGRlVMELyDDVV 29
AtCyp20-3 FSGVYATTKHQRTACVKlSMAlEEEEVlEPQAKVTNKVYFDVElGGEVAGRlVMGLFGEVV 120
          .*:***: :.*: **: : * : : *

HsCypA PKTAENFRAlSTGEKGFg-----YKGSfFHRIlPGFMlQGGDFTRHNGTGGKSlYGEK 82
CeCyp3 PKTAGNFRAlCTGENGIGKSGKPLHFKGSKFHRIlPNFMIQGGDFTRGNGTGGESlYGEK 89
AtCyp20-3 PKTVENFRAlCTGEKKYg-----YKGSsFHRIlKDFMIQGGDFTEGNGTGGISlYGAk 173
***. *****.***: * :*** ***** .** *****. ***** ***** *

HsCypA FEDENfIlKHTGPGlLSMANAGPNTNGSQFFlCTAKTEWLDGKHVVfGKVKEGMNlVEAM 142
CeCyp3 FPDENfKekHTGPGVlLSMANAGPNTNGSQFFlCTVKTEWLDGKHVVfGRVVEGLDVVKAV 149
AtCyp20-3 FEDENfTLKHTGPGlLSMANAGPNTNGSQFFlCTVKTlSWLDNKHVVFgQVIEGMKlVRTL 233
* **** *****:*****:***.***.***.*****:* **:.:.:.:

HsCypA ERfGSRN-GKTSKkITlADCGQLE--- 165
CeCyp3 ESNGSQS-GKPVKDCMIADCGQLKlA-- 173
AtCyp20-3 ESQETRAFdvPKKGCRIYACGELPLDA 260
* :. . . * * **:*
    
```

